Properties of Hyperpolarization-Activated Pacemaker Current Defined by Coassembly of HCN1 and HCN2 Subunits and Basal Modulation by Cyclic Nucleotide

SHAN CHEN,* JING WANG,‡ and STEVEN A. SIEGELBAUM*§‖

From the *Department of Pharmacology, ‡Integrated Program in Cellular, Molecular, and Biophysical Studies, §Center for Neurobiology and Behavior, and ‖Howard Hughes Medical Institute, Columbia University, New York, New York 10032

ABSTRACT   Members of the HCN channel family generate hyperpolarization-activated cation currents (I_h) that are directly regulated by cAMP and contribute to pacemaker activity in heart and brain. The four HCN isoforms show distinct but overlapping patterns of expression in different tissues. Here, we report that HCN1 and HCN2, isoforms coexpressed in neocortex and hippocampus that differ markedly in their biophysical properties, coassemble to generate heteromultimeric channels with novel properties. When expressed in *Xenopus* oocytes, HCN1 channels activate 5–10-fold more rapidly than HCN2 channels. HCN1 channels also activate at voltages that are 10–20 mV more positive than those required to activate HCN2. In cell-free patches, the steady-state activation curve of HCN1 channels shows a minimal shift in response to cAMP (+4 mV), whereas that of HCN2 channels shows a pronounced shift (+17 mV). Coexpression of HCN1 and HCN2 yields I_h currents that activate with kinetics and a voltage dependence that tend to be intermediate between those of HCN1 and HCN2 homomers, although the coexpressed channels do show a relatively large shift by cAMP (+14 mV). Neither the kinetics, steady-state voltage dependence, nor cAMP dose–response curve for the coexpressed I_h can be reproduced by the linear sum of independent populations of HCN1 and HCN2 homomers. These results are most simply explained by the formation of heteromeric channels with novel properties. The properties of these heteromeric channels closely resemble the properties of I_h in hippocampal CA1 pyramidal neurons, cells that coexpress HCN1 and HCN2. Finally, differences in I_h channel properties recorded in cell-free patches versus intact oocytes are shown to be due, in part, to modulation of I_h by basal levels of cAMP in intact cells.

KEY WORDS: potassium channel • gating • heteromultimer • I_h • cAMP

INTRODUCTION

Hyperpolarization-activated cationic currents (I_h)[1] were initially identified in cardiac myocytes (Brown et al., 1979; Brown and DiFrancesco, 1980) and photoreceptors (Bader et al., 1979). These currents (for reviews see DiFrancesco, 1993; Pape, 1996; Santoro and Tibbs, 1999) are characterized by slow activation kinetics upon hyperpolarization, permeability to both K^+ and Na^+, and modulation by direct binding of intracellular cAMP (DiFrancesco and Tortora, 1991), which shifts activation to more positive potentials. In addition to maintaining the resting potential, I_h has been implicated in cardiac (DiFrancesco, 1993) and neuronal (McCormick and Pape, 1990; Pape, 1996) rhythmogenesis, sensory adaptation (Luthi and McCormick, 1998; Demontis et al., 1999), shaping of synaptic potentials (Magee, 1999), and control of synaptic transmitter release (Beaumont and Zucker, 2000; Southan et al., 2000). Reflecting this wide range of physiological functions, the properties of I_h recorded in various tissues differ significantly in their voltage dependence, activation kinetics, and sensitivity to cAMP (Pape, 1996; Santoro and Tibbs, 1999).

The recent cloning of a family of four mammalian genes encoding hyperpolarization-activated cAMP-regulated cation (HCN) channels (Santoro et al., 1997, 1998; Ludwig et al., 1998) provides a potential molecular basis for the heterogeneity in I_h among different cells. The four genes (HCN1–4) encode highly similar proteins that belong to the voltage-gated K channel superfamily (Jan and Jan, 1997): they contain six transmembrane segments, a pore-forming P region, and cytosolic NH_2 and COOH termini. The COOH terminus of the HCN channels also contains a cyclic nucleotide binding domain (CNBD) homologous to those of other cyclic nucleotide binding proteins, including the cyclic nucleotide–gated channels of photoreceptors and olfactory neurons (Zagotta and Siegelbaum, 1996). HCN1–4 also show distinct but overlapping patterns of mRNA expression (Santoro et al., 1997, 1998, 2000;

S. Chan and J. Wang contributed equally to this work.

[1]*Abbreviations used in this paper:* CNBD, cyclic nucleotide binding domain; HCN, hyperpolarization-activated cAMP-regulated cation; I_h, hyperpolarization-activated cationic currents.

Ludwig et al., 1998; Moosmang et al., 1999; Monteggia et al., 2000). All four genes are expressed in brain; HCN2 and HCN4 are also prominently expressed in heart (Ludwig et al., 1998, 1999; Santoro et al., 1998; Shi et al., 1999). HCN1 is expressed selectively in specific brain regions, including hippocampus, layer 5 cells of neocortex, and Purkinje cells of the cerebellum (Santoro et al., 1997, 1998, 2000; Moosmang et al., 1999; Monteggia et al., 2000). HCN2 is widely expressed throughout brain, including neocortex, hippocampus, and thalamus. Finally, HCN4 is expressed in a restricted manner in subcortical and lower brain regions (Santoro et al., 1997, 2000; Moosmang et al., 1999; Monteggia et al., 2000).

When expressed in heterologous systems, three of the four HCN genes have been shown to generate hyperpolarization-activated currents with distinct biophysical properties. HCN1 channels activate fastest and require the least amount of hyperpolarization to open (Santoro et al., 1998, 2000). HCN2 channels activate more slowly, require stronger hyperpolarizations, but are strongly modulated by cAMP (Ludwig et al., 1998, 1999; Santoro et al., 2000). HCN4 may activate at even more negative potentials and with the slowest kinetics (Ishii et al., 1999; Ludwig et al., 1999; Seifert et al., 1999). To date, HCN3 channels have not been found to form functional homomultimers.

Although the recombinant HCN channels and native I_h currents share basic properties, it has not yet been shown whether any HCN homomeric channel can fully reproduce the characteristics of any native I_h current. Since multiple HCN isoforms may be coexpressed in the same cell (Santoro et al., 2000; Franz et al., 2000), this raises the possibility that certain native I_h currents may be generated through the coassembly of HCN isoforms to form heteromeric channels with novel properties distinct from those of the recombinant, homomeric I_h channels. However, the only study where this question was investigated failed to observe the coassembly of HCN2 and HCN4, which are genes that are coexpressed in both heart and certain brain regions (Ludwig et al., 1999).

To investigate the possible formation and resultant properties of heteromeric I_h channels, we coinjected cRNAs encoding mouse isoforms of HCN1 and HCN2, which are coexpressed in neocortical and hippocampal neurons, in *Xenopus* oocytes. I_h generated by coexpression of HCN1 and HCN2 subunits was clearly distinct from I_h generated by homomeric HCN1 or HCN2 channels, providing strong evidence for the formation of heteromultimeric I_h channels with novel properties. In the course of these experiments, we further noticed significant differences between I_h recorded in intact oocytes versus cell-free patches. By making a point mutation in the CNBD to prevent cAMP modulation, we demonstrated that at least a part of these differences is due to

the modulation of I_h in intact oocytes by basal levels of cAMP. Thus, these results suggest that properties of I_h in native neurons and cardiac cells are likely to be determined by both coassembly of distinct HCN subunits and basal modulation by resting levels of cyclic nucleotide.

MATERIALS AND METHODS

Molecular Biology

Mouse HCN1 (Santoro et al., 1998) and HCN2 (Ludwig et al., 1998) were subcloned into the pGHE expression vector. HCN1/R538E and HCN2/R591E, in which arginine 538 of HCN1 or R591 of HCN2 was replaced by glutamate (see Fig. 7 A) were made by a PCR/subcloning strategy. The resulting mutant HCN channels were verified by dideoxy chain termination sequencing.

Expression in Xenopus Oocytes

RNA was transcribed from NheI-linearized DNA (HCN1) or SphI-linearized DNA (HCN2) using a T7 RNA polymerase (Message Machine; Ambion) and injected into *Xenopus* oocytes as described previously (Goulding et al., 1992; Santoro et al., 1998). In the case of inside-out patches, the oocytes were injected with 50 ng of cRNA of either HCN1 or HCN2 alone, with a combination of 25 ng of HCN1 cRNA and 25 ng of HCN2 cRNA for coexpression, or 50 ng of cRNA from mutant constructs HCN1/R538E or HCN2/R591E alone. In the case of two microelectrode voltage-clamp of intact oocytes, the amount of injection is one fifth of that used for inside-out patches.

Electrophysiological Recordings

Two microelectrode voltage-clamp recordings were obtained 1–2 d after cRNA injection using an oocyte clamp amplifier (model OC-725B; Warner Instruments). Data were filtered at 250 Hz and sampled at 500 Hz using an ITC-18 interface and Pulse software (HEKA). The recordings were obtained with the oocytes bathed in a high KCl extracellular solution containing (in mM): 96 KCl, 2 NaCl, 10 HEPES, and 2 MgCl$_2$, pH 7.5. Microelectrodes were filled with 3 M KCl and had resistances of 0.5–2 MΩ. Holding potential was -30 mV. Analysis was done using Pulsefit (HEKA) and IgorPro (WaveMetrics).

Cell-free inside-out patches were obtained 3–6 d after cRNA injection, and data were acquired using a patch-clamp amplifier (model Axopatch 200A; Axon Instruments). A symmetrical solution was used containing (in mM): 107 KCl, 5 NaCl, 10 Hepes, 1 MgCl$_2$, and 1 EGTA, pH 7.3. Patch pipets were 1–3 MΩ, and were coated with Sylgard to minimize capacitance. The holding potential for these inside-out patches was -40 mV. A Ag-AgCl ground wire was connected to the bath solution by a 3-M KCl agar bridge electrode, and junction potential was compensated before the formation of each patch. Linear leak was not subtracted. Acquired data were filtered at 1 kHz with the Axopatch 200A built-in 4-pole low pass Bessel filter and sampled at 2 kHz with an ITC-18 interface. Analysis was done using PulseFit, IgorPro, and Sigma Plot.

Hyperpolarizing voltages in 10- or 5-mV step increments were applied to either inside-out patches or intact oocytes from the holding potential. All recordings were obtained at room temperature (22–25°C).

Data Analysis

Steady-state activation curves were determined from the amplitude of tail currents after hyperpolarizing steps on return to -40 mV. Tail current amplitudes were measured after the decay of the capacitive transient by averaging the current during the plateau

of the tail. Current values were plotted as a function of the step voltages and fit with the Boltzmann equation: $I(V) = A_1 + A_2/\{1 + \exp[(V - V_{1/2})/s]\}$, where A_1 is an offset caused by a nonzero holding current, A_2 is the maximal tail current amplitude, V is voltage during the hyperpolarizing test pulse in mV, $V_{1/2}$ is the midpoint activation voltage, and s is the slope of fitting. To average the data from different experiments, the tail current amplitudes for each individual experiment were normalized by first subtracting the fitted value of A_1, and then dividing by the fitted value of A_2. These normalized data were averaged among the different experiments and the averaged, normalized data were then fitted by the Boltzmann equation with A_1 set to 0 and A_2 set to 1. These normalized curves were plotted in the indicated figures.

Activation time constants were determined by fitting the current evoked during hyperpolarizing voltage steps to single or double exponential functions using Pulsefit. Simultaneous fitting with two exponential components yielded fits that were significantly better than single exponential terms for all currents activated in response to voltages that were negative to $V_{1/2}$; for all the currents including the coexpression of two HCN channels, the fit was not improved after addition of a third component. The uncompensated capacitive transients and activation delays occurring in the initial phase of the I_h currents (initial 50–100 ms) were excluded from the fitting windows. Data are presented as mean ± SEM.

R E S U L T S

The properties of hyperpolarization-activated currents upon coexpression of HCN1 and HCN2 subunits were compared with the I_h currents generated upon expression of HCN1 or HCN2 alone. If the two subunits did indeed coassemble to form a heteromultimer with novel properties, we expected that the heteromultimeric I_h would not be adequately described by the algebraic sum of two independent populations of HCN1 and HCN2 channels, at any proportional ratio.

In Intact Oocytes, Coexpression of HCN1 and HCN2 Generates an I_h with Novel Properties

We first characterized properties of I_h generated by expression of HCN1 alone, HCN2 alone, or coexpression of the two isoforms in intact oocytes using two microelectrode voltage-clamp. As reported previously (Santoro et al., 1998, 2000), HCN1 currents activated relatively rapidly upon hyperpolarization, with no pronounced sigmoidal delay at the beginning of the step, and generally reached steady-state activation within a few hundred milliseconds. By contrast, HCN2 currents activated very slowly, with a distinct sigmoidal onset contributing to an initial delay. After the initial delay, HCN2 channels required up to 10–30 s to reach steady-state activation at the less negative voltages (Figs. 1 A and 2 B). Oocytes coinjected with HCN1 and HCN2 cRNA expressed currents that activated without a noticeable delay and showed intermediate kinetics that were faster than those of HCN2, but slower than those of HCN1.

The time course of I_h upon coexpression of HCN1 and HCN2 subunits could not be reproduced by the algebraic sum of independent populations of homo-meric HCN1 and HCN2 channel currents, suggesting the formation of heteromultimeric I_h currents with distinct properties (Fig. 1 B). To characterize the properties of the coexpressed channels, we fit the time course of I_h activation with two exponential components (Fig. 2 A), which were necessary and sufficient to describe adequately the activation kinetics of the coexpressed currents as well as the kinetics of HCN1 or HCN2 homomultimers (Santoro et al., 2000).

For all recombinant I_h studied, the fast and slow exponential components (τ_f and τ_s) were voltage-dependent, speeding up at more hyperpolarized voltages. Over the entire voltage range of activation, the fast and slow time constants of activation for HCN1 were ~10-fold more rapid than the respective time constants for HCN2 (Santoro et al., 2000). In general, the fast and slow time constants of the coexpressed I_h were intermediate between those of I_h generated by HCN1 alone and HCN2 alone. At more depolarized voltages, both fast and slow time constants for the coexpressed I_h lay somewhat closer to the values for HCN1 homomers than to HCN2 homomers (Fig. 2 B).

The voltage dependence of the relative amplitudes of the fast and slow exponential components differs significantly between HCN1 and HCN2 homomeric channels (Santoro et al., 2000). For HCN1 channels, the fast component of activation accounted for the great majority (~80%) of the current amplitude, and this proportion did not depend on the voltage during the hyperpolarization. In contrast, for HCN2 channels, the slow component was predominant for relatively small hyperpolarizations, where less than half the channels open. At more hyperpolarized voltages, the contribution of the fast component for HCN2 became progressively greater. The relative amplitude of the fast and slow exponential components of I_h generated by coexpression of HCN1 and HCN2 showed a marked dependence on voltage that was similar to, but slightly less steep than, the behavior of HCN2 channels (Fig. 2 B).

Examination of the steady-state voltage dependence of channel activation further supported the view that HCN1 and HCN2 subunits formed heteromultimeric channels. Tail current activation curves were measured for I_h generated by expression of HCN1 alone, HCN2 alone, and coexpression of HCN1 and HCN2 (Fig. 3). As shown previously (Santoro et al., 2000), HCN1 channels tend to activate at more positive voltages than HCN2 channels. Fits of the Boltzmann relation to activation curves showed that the midpoint voltage of activation ($V_{1/2}$) of HCN1 was −69.1 ± 0.7 mV with a slope of 7.5 ± 0.5 mV ($n = 8$). In comparison, HCN2 channels showed a more negative $V_{1/2}$ of −78.4 ± 0.8 mV with a slope of 5.1 ± 0.4 mV ($n = 8$). Surprisingly, channels generated by coinjection of HCN1 and HCN2 showed steady-state activation parameters almost iden-
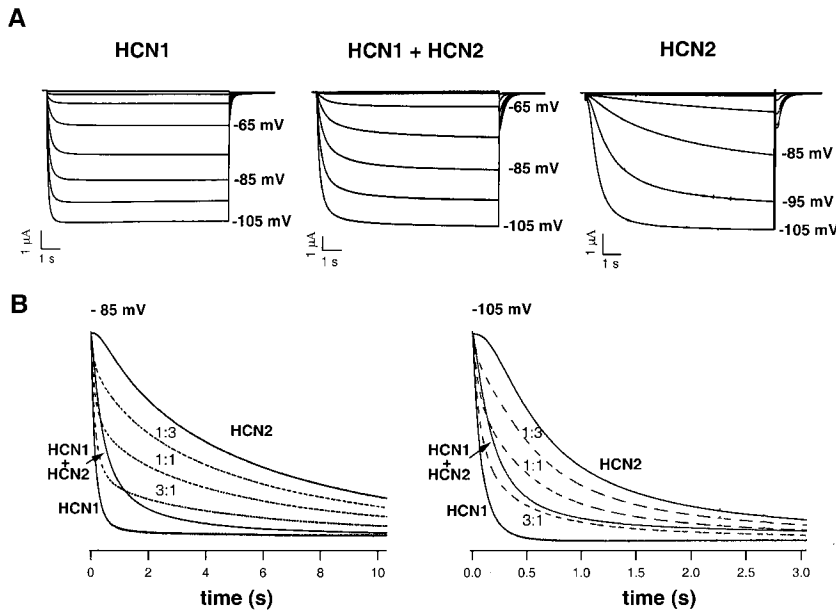
FIGURE 1. Coexpression of HCN1 and HCN2 results in currents recorded from intact oocytes with novel kinetics that cannot be accounted for by expression of two independent populations of homomeric HCN channels. (A) Currents recorded by two microelectrode voltage clamp elicited by 10-s hyperpolarizations in oocytes injected with cRNA of either HCN1 (left), HCN2 (right) alone, or with a 1:1 mixture of HCN1 and HCN2 (HCN1 + HCN2) (middle). Holding potential was −30 mV, and the voltage was stepped to negative potentials from −35 mV in 10-mV increments to −105 mV. Tail currents were measured at −40 mV. (B) Current traces elicited by 30-s pulses to −85 mV (bottom left) or 10-s pulses to −105 mV (bottom right) from oocytes injected with HCN1 alone, HCN2 alone, or 1:1 mixture of HCN1 and HCN2 (HCN1 + HCN2). Solid traces show normalized averaged currents from several oocytes injected with given composition of RNA. Dashed traces show algebraic sums of HCN1 and HCN2 averaged currents in ratios of 1:3, 1:1, and 3:1 (HCN1/HCN2 ratio). Four to five separate experiments (oocytes) averaged for each recording trace.
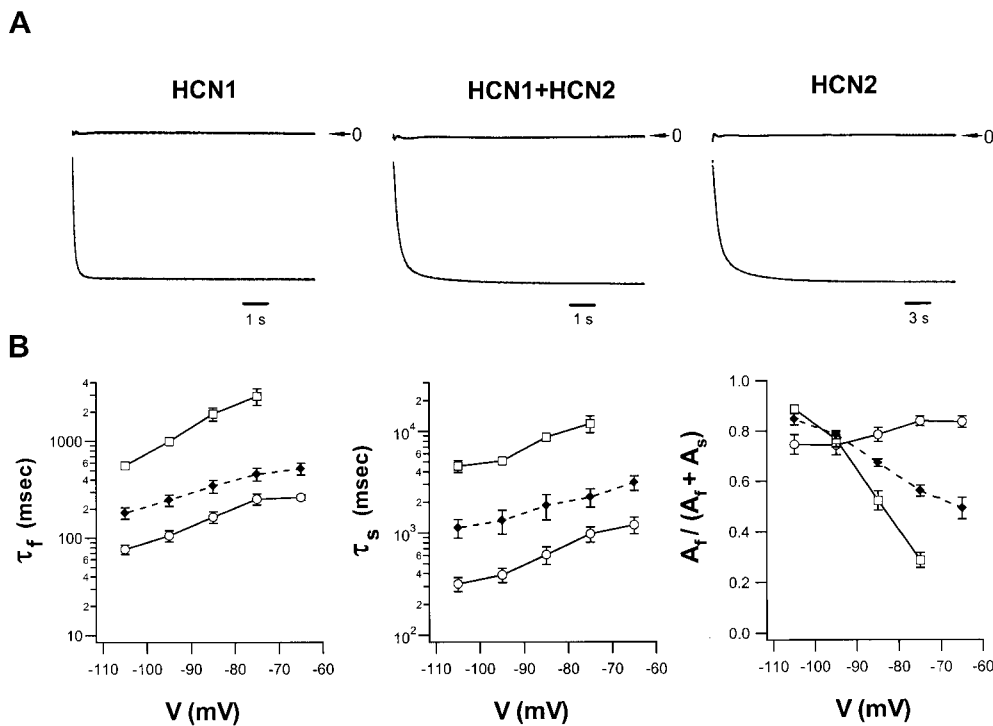

FIGURE 2. Activation kinetics for HCN1, HCN2, and coexpressed subunits from intact oocytes. (A) I_h currents during hyperpolarizing steps to −105 mV with superimposed fit of sum of two exponential functions (bottom traces) with residuals showing difference between data and fit (top traces). (left) HCN1 alone (10-s step); (middle) HCN1 + HCN2 (10-s step); and (right) HCN2 alone (30-s step). (B) Plot of two exponential constants as function of voltage. (left) Voltage dependence of fast exponential time constant (τ_f). (middle) Voltage dependence of slow exponential time constant (τ_s). (right) Relative amplitude of fast exponential component as function of voltage, $A_f/(A_f + A_s)$, where A_f and A_s are the amplitudes of the fast and slow exponential components, respectively. (open circles) HCN1; (open squares) HCN2; (closed diamonds) HCN1 + HCN2.

A

HCN1   HCN1 + HCN2   HCN2
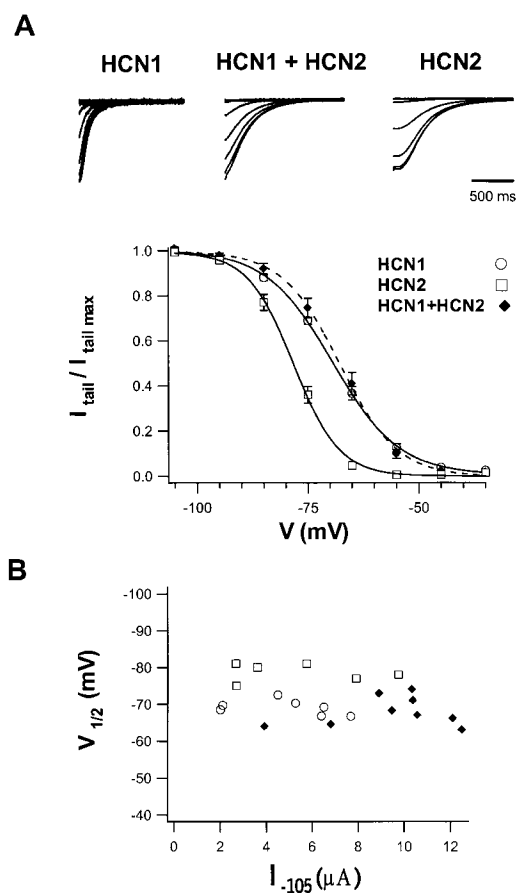
500 ms

HCN1 ○
HCN2 □
HCN1+HCN2 ◆

B

FIGURE 3. Steady-state activation curves for HCN1, HCN2, and coexpressed channels in intact oocytes. (A, top) Tail currents of either HCN1 alone, HCN2 alone, or coinjected HCN1 and HCN2. (bottom) Averaged, normalized steady-state tail current activation curves were obtained using 10-s hyperpolarizing steps for HCN1 currents (open circles, 8 cells) and currents produced by coexpression of HCN1 and HCN2 (closed diamonds, 9 cells); 30-s hyperpolarizing steps were used for HCN2 currents (open squares, 8 cells). Curves show fit of Boltzmann relations (see MATERIALS AND METHODS for details). Bars show SEM. (B) Relation of steady-state $V_{1/2}$ and I_h current amplitude at the end of 3-s hyperpolarizing step to −105 mV. Each symbol shows data recorded for an individual oocyte injected with HCN1 (open circles), HCN2 (open squares), or HCN1 + HCN2 (closed diamonds).

tical to those of HCN1, with a $V_{1/2}$ value of −68.0 ± 1.4 mV and a slope of 6.1 ± 0.4 mV ($n = 9$). The fact that the steady-state activation curve observed upon coexpression of HCN1 and HCN2 resembles the HCN1 activation curve cannot be explained by a lack of expression of HCN2 subunits because the coexpressed channels show markedly slower kinetics of activation (Figs. 1 and 2) and tail current deactivation (Fig. 3 A, top traces) compared with HCN1 homomers. Moreover, we find that the $V_{1/2}$ values for HCN1 homomers, HCN2 homomers, and coexpressed channels are independent of the magnitude of the I_h current (Fig. 3 B), suggesting a lack of competition among the various subunits for some limiting factor in the oocytes.

Coexpression of HCN1 and HCN2 Studied in Inside-out Patches: Novel Gating and Modulation by cAMP

The effects of cAMP on HCN channel function were measured using cell-free inside-out patches, which permitted the rapid application of solutions to the internal face of the membrane. As previously reported for I_h in cardiac myocytes (DiFrancesco and Mangoni, 1994), we found that loss of intracellular constituents upon patch excision shifted the relation between channel opening and voltage by 40–60 mV in the hyperpolarizing direction for both HCN1 and HCN2 channels. Nonetheless, the essential differences in gating kinetics between HCN1 and HCN2 were maintained in the cell-free patches (Fig. 4 A). Thus, HCN1 channels activated at more positive potentials and with more rapid kinetics compared with HCN2 channels. The difference in kinetics was clearly observed during steps to −135 mV; HCN1 currents reached steady-state activation in <300 ms, whereas HCN2 currents did not reach full activation even after 3 s (Fig. 4 C). In cell-free patches, the I_h current generated by coexpression of HCN1 and HCN2 displayed intermediate activation kinetics, similar to our findings in intact oocytes. During steps to −135 mV, steady-state activation was reached in ∼3s.

The effects of application of a saturating concentration of cAMP were studied for I_h generated by HCN1 alone, HCN2 alone, and by coexpression of HCN1 and HCN2 (Fig. 4, B and C). Similar to previous findings, cAMP caused only a small increase in the rate of activation of HCN1 channels (Santoro et al., 1998). In contrast, there was a large increase in the rate of activation of HCN2, over the entire voltage range examined (Ludwig et al., 1998). Channels generated by the coexpression of HCN1 and HCN2 showed a marked enhancement in the rate of opening with cAMP, similar to (although somewhat less than) the speeding of HCN2 channels.

The effects of cAMP on the voltage dependence of gating were examined next using tail current activation curves (Fig. 5 and Table I). In the absence of cAMP, HCN1 activated at voltages that were 20 mV more positive than those required to activate HCN2 channels. For HCN1, the $V_{1/2}$ of activation was −115.8 ± 1.3 mV with a slope of 6.3 ± 0.7 mV. For HCN2, the $V_{1/2}$ was −135.7 ± 1.7 mV with a slope of 4.3 ± 0.3 mV. Thus, although $V_{1/2}$ values were shifted by ∼50 mV relative to their values in intact oocytes, the qualitative difference in voltage dependence between HCN1 and HCN2 was maintained in the inside-out patches. In fact, the 20-mV difference in $V_{1/2}$ between HCN1 and HCN2 in cell-free patches was larger than the 10-mV difference observed in intact oocytes.

Channels generated by the coinjection of HCN1 and HCN2 showed an intermediate voltage dependence of activation, with a $V_{1/2}$ of −129.7 ± 1.1 mV and a slope of
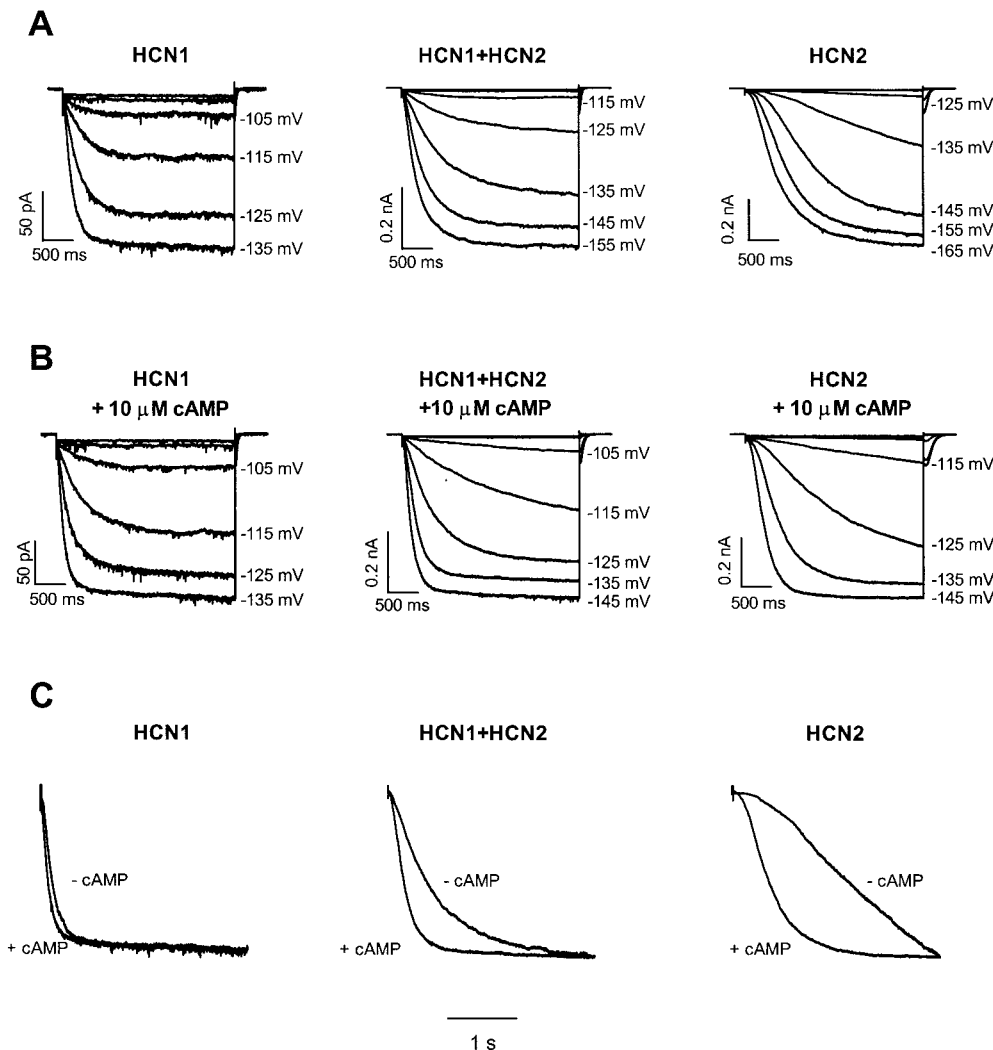
FIGURE 4. Coexpression of HCN1 and HCN2 gives rise to a distinct I_h phenotype in inside-out patches. (A) Currents elicited by 3-s hyperpolarizations in patches obtained from oocytes injected with cRNA of either HCN1 alone (left), HCN2 alone (right), or with a 1:1 mixture of HCN1 and HCN2 (HCN1 + HCN2) (middle). Patches were stepped to voltages ranging from −85 to −165 mV in 10-mV steps from a holding potential of −40 mV. (B) Effect of cAMP on channel activation. Currents shown for same patches with same protocols as in A, but in the presence of 10 μM cAMP. (c) Activation kinetics during a step to −135 mV in the presence and absence of 10 μM cAMP. Superimposed traces shown in A and B were scaled so amplitudes were equaled.

4.4 ± 0.5 mV (Fig. 5 A and Table I). This result is somewhat surprising given the results presented above that, in intact oocytes, the $V_{1/2}$ of the coexpressed channels was similar to that of HCN1, not intermediate between HCN1 and HCN2. The explanation for this discrepancy, as well as the greater difference in $V_{1/2}$ between HCN1 and HCN2 homomeric channels in inside-out patches versus intact oocytes, is explored below.

Further evidence that I_h generated by coexpression of HCN1 and HCN2 subunits reflected the novel properties of heteromeric channels was provided by comparison of experimental and simulated tail current activation curves (Fig. 5). The activation data for I_h measured in patches from oocytes in which HCN1 and HCN2 were coexpressed (either for I_h from a single, representative patch [Fig. 5 B], or averaged from seven separate patches [Fig. 5 C]) could not be accounted for by the sum of activation curves for independent populations of HCN1 and HCN2 channels at varying proportions.

Because of the quantitative difference in the response of HCN1 versus HCN2 homomeric channels to

cAMP, we next examined the effect of this nucleotide on the gating of the coexpressed HCN channels (Fig. 5 and Table I). As previously shown, a saturating concentration of cAMP (10 μM) shifted the $V_{1/2}$ of HCN1 channels by only ~4 mV (similar to the findings of Santoro et al., 1998). In contrast, application of cAMP shifted the $V_{1/2}$ of HCN2 channels by a much larger amount, ~17 mV (similar to the findings of Ludwig et al., 1998). The coexpressed channels showed a 13-mV shift in $V_{1/2}$ in response to 10 μM cAMP, which is close to the large shift seen in HCN2 channels.

Dose–response relations for the shift in $V_{1/2}$ as a function of [cAMP] were compared for HCN1, HCN2, and coexpressed channels (Fig. 6). The dose–response curves were fitted by the Hill equation to obtain the maximal shift at saturating [cAMP], the cAMP concentration at which half of the maximal shift was produced ($K_{1/2}$), and the Hill coefficient (h). For HCN2 channels, the maximal shift with cAMP was 17.4 mV with a $K_{1/2}$ of 0.10 μM (h = 1.1). For HCN1 channels, the shift was only 4.1 mV with a $K_{1/2}$ of 0.06 μM (h = 1.0).

Tail Current Activation Parameters

Clones	Intact Oocytes (2 M.E.)			I.O. Patch no cAMP			I.O. Patch + 10 μM cAMP	
	$V_{1/2}$	Slope	n	$V_{1/2}$	Slope	n	$V_{1/2}$	Slope
	(mV)	*(mV)*		*(mV)*	*(mV)*		*(mV)*	*(mV)*
HCN1	-69.1 ± 0.7	7.5 ± 0.5	8	-115.8 ± 1.3	6.3 ± 0.7	7	-111.2 ± 1.0	4.9 ± 0.3
HCN1 + HCN2	-68.0 ± 1.4	6.1 ± 0.4	9	-129.7 ± 1.1	4.4 ± 0.5	9	-116.7 ± 1.1	5.1 ± 0.1
HCN2	-78.4 ± 0.8	5.1 ± 0.4	8	-135.7 ± 1.7	4.3 ± 0.3	10	-119.0 ± 1.7	4.3 ± 0.2
HCN1/R538E	-75.9 ± 1.0	6.1 ± 0.3	10	-116.3 ± 1.8	5.2 ± 0.3	7	-117.1 ± 1.9	5.3 ± 0.2
HCN1 + 2/RE	-81.8 ± 1.6	6.7 ± 0.3	9	ND	ND		ND	ND
HCN2/R591E	-97.1 ± 0.9	5.0 ± 0.3	9	-136.1 ± 2.2	3.4 ± 0.3	5	-136.7 ± 3	3.3 ± 0.5

Data obtained from fits of Boltzmann Eq. to mean, normalized tail current activation curves. HCN1+HCN2 data obtained from coexpression of HCN1 and HCN2. HCN1 + 2/RE data obtained from coexpression of HCN1/R538E and HCN2/R591E mutant subunits.

Thus, the small effect of cAMP on HCN1 gating does not reflect a low sensitivity to the ligand. Finally, for channels formed by coexpression, the maximal shift was 14.0 mV with a $K_{1/2}$ of 0.19 μM (h = 1.3). Surprisingly, the $K_{1/2}$ for channels generated by coexpression was greater than the $K_{1/2}$ for either of the homomeric channels. Furthermore, the dose–response curve for the coexpressed channels could not be reproduced by the sum of independent populations of homomeric HCN1 and HCN2 channels (Fig. 6).
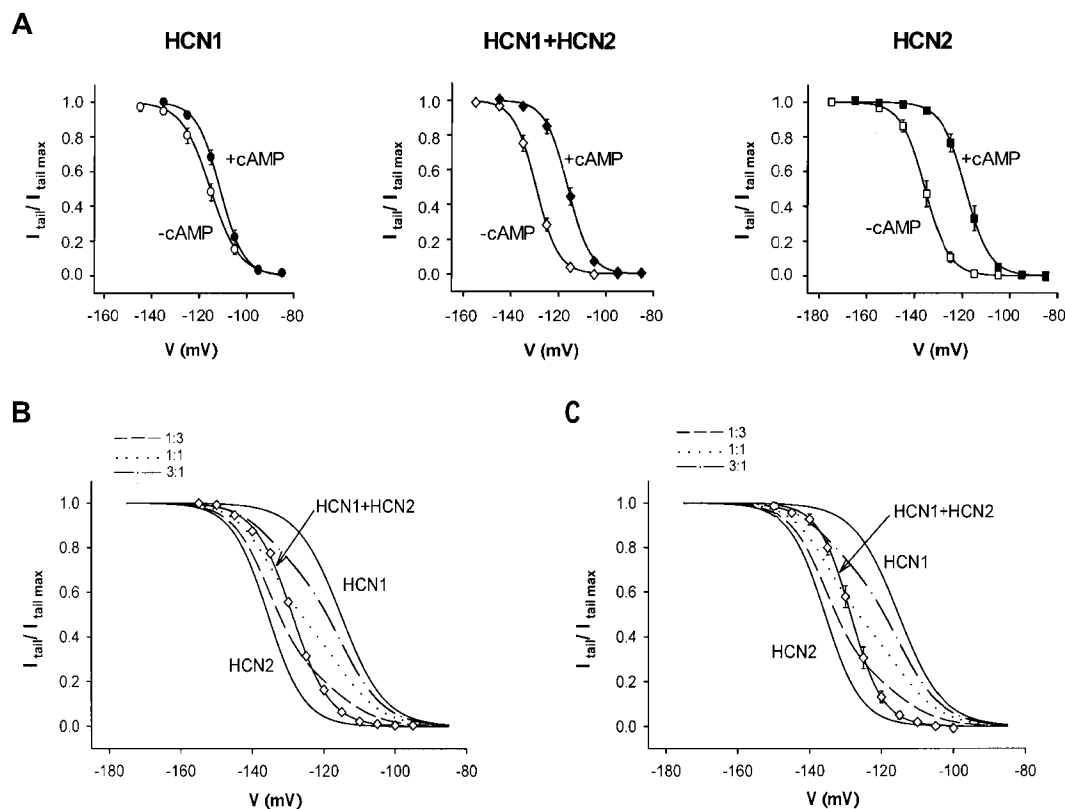

FIGURE 5. Steady-state activation curves determined in inside-out patches in the presence and absence of cAMP. (A) Average tail current activation curves for HCN1, HCN2, and coexpression of HCN1 and HCN2 in the presence (closed symbols) and absence (open symbols) of 10 μM cAMP. (left) HCN1 (7 patches); (middle) coexpression of HCN1 and HCN2 (9 patches); (right) HCN2 (10 patches). Solid lines show fit of Boltzmann relation. (B) The activation curve of I_h current generated by coexpression of HCN1 and HCN2 from a representative patch cannot be reproduced by linear sums of average HCN1 and HCN2 activation curves obtained from A. (solid lines) HCN2, HCN1 + HCN2 (open diamonds), and HCN1 from left to right. Dashed, dotted, and dash-dotted lines: linear sums of HCN1 and HCN2 activation curves at 1:3, 1:1, 3:1 (HCN1/HCN2) ratios. (C) The average Boltzmann activation curve for I_h currents generated by coexpression of HCN1 and HCN2 (open diamonds, 7 patches) cannot be reproduced by linear sums of average HCN1 and HCN2 activation curves. Bars indicate SEM.
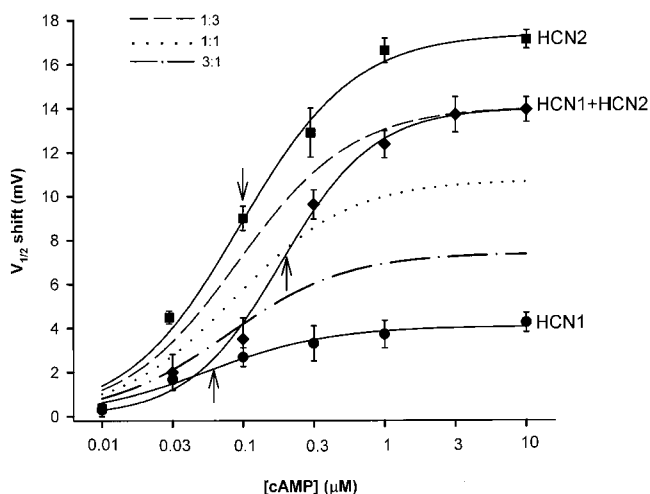
FIGURE 6. Coexpression of HCN1 and HCN2 generates channels with a novel cAMP dose–response relation. Mean dose–response curves for shifts in $V_{1/2}$ as a function of cAMP concentration for HCN1 (closed circles, 26 patches), HCN2 (closed squares, 16 patches), and coexpression of HCN1 and HCN2 (closed diamonds, 31 patches). Solid lines show fit of the Hill equation (see MATERIALS AND METHODS). The positions of the $K_{1/2}$ values are indicated by arrows. Dash, dotted, and dash-dotted lines: linear sums of HCN1 and HCN2 dose–response curves at 1:3, 1:1, 3:1 (HCN1/HCN2) ratios.

Modulation of HCN Channels by Basal cAMP in Intact Oocytes Studied through an Inactivating Point Mutation in the Cyclic Nucleotide Binding Domain

Although the above results in intact oocytes and cell-free patches supported the view that HCN1 and HCN2 subunits coassemble to form heteromultimeric channels with novel properties, there were certain puzzling differences in the behavior of the various channels in the two recording configurations. First, we found a large, ~50-mV hyperpolarizing shift in $V_{1/2}$ values measured for I_h in cell-free patches relative to values in intact oocytes. Moreover, we found a larger difference in $V_{1/2}$ values between HCN1 channels and HCN2 channels in cell-free patches (20 mV) than in intact oocytes (9 mV). Finally, in cell-free patches, the $V_{1/2}$ of coexpressed channels was intermediate between the $V_{1/2}$ values for channels formed by HCN1 or HCN2 alone. In contrast, in intact oocytes, the $V_{1/2}$ for coexpressed channels was similar to that of HCN1 channels. What might account for such differences?

Given the high sensitivity of HCN channels to cAMP, we investigated whether basal levels of cAMP in the intact oocytes might have been sufficient to modulate the gating of HCN channels. To investigate this possibility, we mutated a single arginine residue (R538 in HCN1 and R591 in HCN2) that is conserved in nearly all
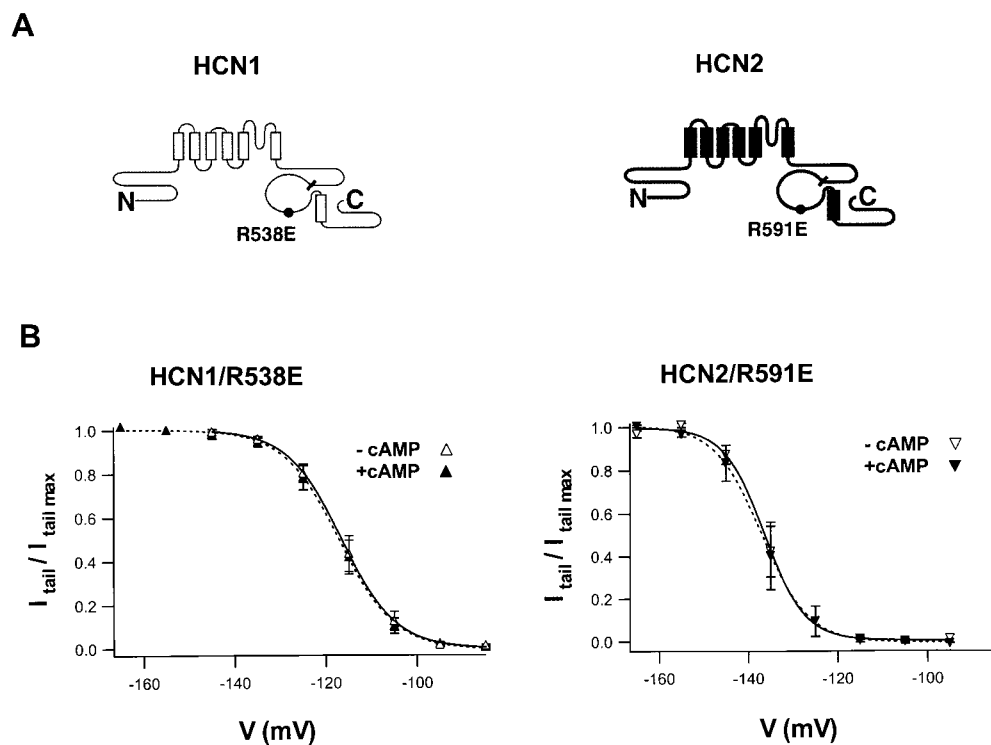

FIGURE 7. Mutation of a conserved arginine residue in the CNBD to glutamate prevents cAMP binding, but has no effect on the channel's intrinsic voltage dependence. (A) Diagram showing the site of the mutation. HCN1 and HCN2 are shown as six transmembrane helices (rectangles) with the P-loop connecting the fifth and sixth helices. The CNBD, located in the cytoplasmic COOH terminus, starts at the hash mark and ends at the last rectangle. It is depicted as a loop, representing the β-roll, and a rectangle, representing the C α-helix. (B) Steady-state tail current activation curves obtained in inside-out patches using 3-s hyperpolarizing steps for HCN1/R538E (left) and HCN2/R591E (right) channels. (open symbols) Data in absence of cAMP. (closed symbols) Data in presence of 10 μM cAMP. Solid and dashed curves show fits of Boltzmann relation in absence and presence of cAMP, respectively (see Table I for values).
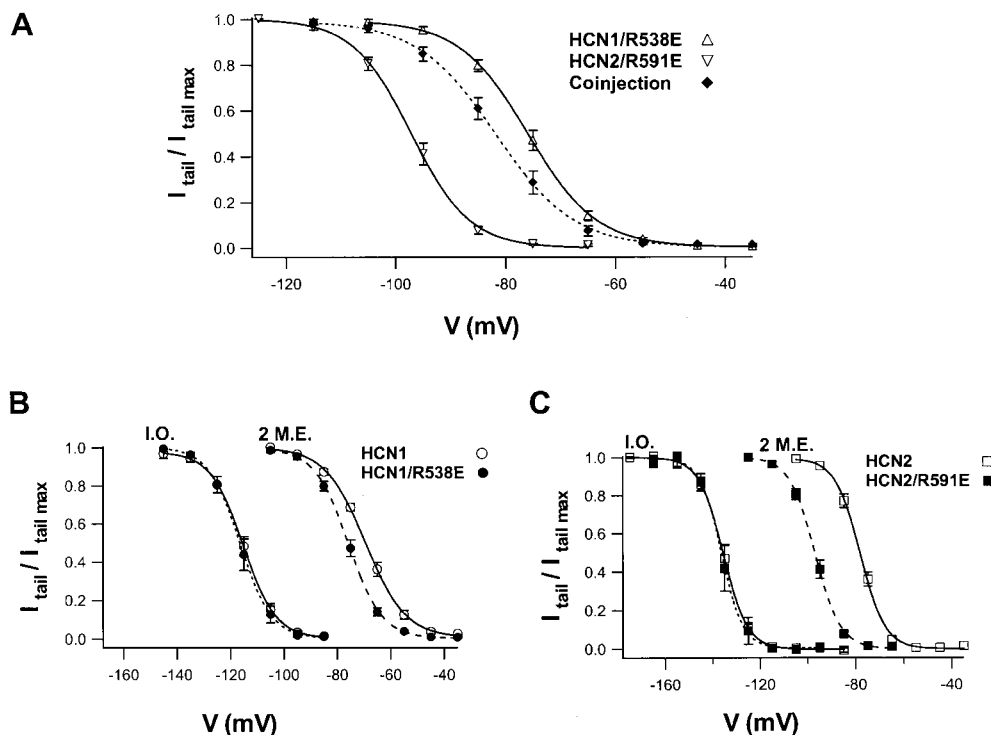
FIGURE 8. Comparison of effects of the arginine to glutamate point mutation on HCN channels in inside-out patches versus intact oocytes. (A) Mean steady-state tail current activation curves in intact oocytes using two microelectrode voltage clamp for HCN1/R538E channels (triangles), HCN2/R591E channels (inverted triangles), or channels formed upon coinjection of the two mutant subunits (closed symbol). Tail currents obtained after 10-s hyperpolarizing steps. (B and C), Comparisons of steady-state activation curves for wild-type (open symbols) versus mutant (closed symbols) HCN1 (B) or HCN2 (C) subunits in inside-out patches (I.O.) and intact oocytes studied with two microelectrode voltage-clamp (2 M.E.). Solid and dashed lines show fits of Boltzmann relation to wild-type and mutant subunits, respectively.

CNBDs (Shabb and Corbin, 1992; Santoro and Tibbs, 1999) to a glutamate (Fig. 7 A). In related CNBDs this arginine, which is located in an eight-stranded antiparallel β-roll, makes a crucial ionic contact with the cyclized phosphate of the bound nucleotide (Weber and Steitz, 1987; Su et al., 1995). In the CNG channels, mutation of this arginine to glutamate decreases the affinity of the channel for cyclic nucleotide by >2,000-fold without affecting the energetics of the intrinsic gating reaction (Tibbs et al., 1998).

In the background of both HCN1 and HCN2 channels, the arginine (R) to glutamate (E) mutation had a very similar effect as in CNG channels. Thus, the gating of mutant HCN1/R538E and HCN2/R591E homomeric channels in inside-out patches was completely unaffected by 10 μM cAMP (Fig. 7, B and C, and Table I), which is a concentration that is 50–100-fold higher than the $K_{1/2}$ for modulation of wild-type HCN channels. However, the mutation had no effect on the intrinsic gating properties of the channels, as shown by the nearly identical activation curves of wild-type and mutant channels in the absence of cAMP (Table I and Fig. 8, B and C).

In contrast to the lack of effect of these mutations on HCN gating in cell-free patches, in intact oocytes studied by two microelectrode voltage-clamp, we observed a pronounced negative shift in the gating of HCN1/R538E channels, HCN2/R591E channels, and coexpressed mutant channels relative to the gating of the respective wild-

type channels. Thus, the $V_{1/2}$ of HCN1/R538E was −75.9 ± 1.0 mV with a slope of 6.1 ± 0.3 mV ($n = 10$ cells), representing a shift of about −7 mV compared with wild-type HCN1 channels (Fig. 8 B). The $V_{1/2}$ of HCN2/R591E was −97.1 ± 0.9 mV with a slope of 5.0 ± 0.3 ($n = 9$), representing a shift of about −19 mV compared with wild-type HCN2 (Fig. 8 C). Finally, the $V_{1/2}$ of the currents from oocytes coinjected with HCN1/R538E and HCN2/R591E was −81.8 ± 1.6 mV with a slope of 6.7 ±0.3 (from 10 cells), representing a shift of −14 mV (comparing Fig. 3 with Fig. 8 A). These shifts in $V_{1/2}$ values for HCN1/R538E (7 mV), HCN2/R591E (19 mV), and coexpressed mutant subunits (14 mV) in intact oocytes are compatible with the maximal shifts of 4, 17, and 14 mV seen in response to cAMP in inside-out patches for channels formed by the corresponding wild-type HCN channels. Thus, our results are consistent with the view that basal levels of cAMP were sufficient to cause a maximal positive voltage shift in the gating of HCN channels in intact oocytes. Differences in efficacy of cAMP in modulating HCN1, HCN2, and HCN1/HCN2 heteromultimers could explain some of the discrepancies between I_h properties recorded from inside-out patches versus intact oocytes (Fig. 8, B and C).

DISCUSSION

Our study in both intact *Xenopus* oocytes and inside-out patches demonstrated that HCN1 and HCN2 subunits,

when coexpressed, form functional heteromultimeric channels that generate hyperpolarization-activated currents with novel properties. Furthermore, we showed that the basal level of cAMP may play an important role in the modulation of HCN channel function in intact cells. Both coassembly and basal cAMP modulation significantly increase the potential for functional diversity of I_h in the nervous and cardiovascular systems.

Formation of Heteromultimers between Two Different Isoforms of HCN Channels

In situ hybridization studies of mouse brain have revealed distinct but overlapping patterns of expression of HCN1 and HCN2 (Moosmang et al., 1999; Monteggia et al., 2000; Santoro et al., 2000). Single cell PCR studies provide additional strong evidence for coexpression of different HCN isoforms within single neurons (Franz et al., 2000). In particular, both HCN1 and HCN2 are prominently expressed in CA3 and CA1 pyramidal neurons of the hippocampus. Whole-cell patch-clamp recordings demonstrate a prominent I_h current with relatively rapid kinetics in CA1 pyramidal neurons. The presence of multiple HCN isoforms in a given cell raises the question as to whether the I_h current in these cells results from separate populations of homomeric channels or whether the different isoforms coassemble to form heteromultimeric channels.

By coexpressing HCN1 and HCN2 in *Xenopus* oocytes, we have provided several lines of functional evidence that the two isoforms can indeed coassemble to form functional heteromultimers with novel properties. In intact oocytes, coexpression of HCN1 and HCN2 gave rise to I_h with a voltage dependence similar to that of HCN1 channels, but with kinetics that were twice as slow. In inside-out patches, the coexpressed channels displayed a voltage dependence and an efficacy of cAMP modulation that were intermediate between those of HCN1 and HCN2 channels. Simulation of hyperpolarization-activated currents generated by the summed contributions of independent populations of HCN1 and HCN2 channels in various ratios could not reproduce the currents we observed from coinjected oocytes. Finally, the coexpressed channels displayed a decreased sensitivity to cAMP (increased $K_{1/2}$) compared with either HCN1 or HCN2 channels.

Although the hypothesis that HCN1 and HCN2 subunits coassemble to form functional heteromultimeric channels with novel properties provides the simplest explanation for our findings, a number of more complicated scenarios might be envisioned. For example, HCN1 and HCN2 could compete for some limiting cofactor in the oocytes (e.g., a β subunit or modulatory enzyme), so that coexpression of the two subunits leads to a change in the functional properties of homomeric HCN1 and HCN2 channels, relative to their properties when expressed alone. However, the fact that the steady-state activation curves we observe upon coexpression of HCN1 and HCN2 (in both cell-free patches and intact oocytes) is as steep as that observed upon expression of either HCN1 or HCN2 alone argues strongly against the presence of two distinct channel populations (which would inevitably lead to a shallower activation curve, unless the $V_{1/2}$ values just happened to coincide). Furthermore, such a competition for a limiting cofactor is inconsistent with our finding that $V_{1/2}$ values are independent of level of I_h current expression (Fig. 3 B). This latter finding also argues against a change in homomeric channel properties due to some direct interaction between homomeric HCN1 and HCN2 channels.

Further evidence that the properties of the channels observed upon coexpression of HCN1 and HCN2 subunits do indeed reflect the properties of heteromeric channels comes from a recent study of Ulens and Tytgat (2001), in which tandem heterodimers of HCN1 and HCN2 subunits were expressed in *Xenopus* oocytes. The tandem dimers generated functional channels with properties intermediate between those of HCN1 and HCN2 homomeric channels, but very similar to the properties of the channels formed upon coexpression of independent HCN1 and HCN2 subunits that we report here. The two approaches complement one another as each has its own strengths and weaknesses. The tandem dimers might artificially force distinct subunits to coassemble or generate channels with altered properties (e.g., due to the fusion of COOH and NH_2 termini). Independent coexpression of distinct subunits, however, cannot constrain stoichiometry and, therefore, might result in expression of multiple populations of channels. Thus, the good agreement between the two approaches reinforces the conclusion that HCN1 and HCN2 subunits do indeed coassemble to form heteromultimers, and that the properties of the coexpressed channels and tandem dimer channels are an accurate representation of the properties of heteromeric HCN1/HCN2 channels. Moreover, the agreement between the two sets of experiments suggests that the subunit stoichiometry of the heteromeric channels is likely to consist of two HCN1 subunits and two HCN2 subunits.

The only significant quantitative discrepancy between our results and those of Ulens and Tytgat (2001) lies in the extent of modulation of homomeric and heteromeric channels by cAMP. Ulens and Tytgat elevated cAMP levels in oocytes by activation of G protein–coupled receptors. They observed no effect of cAMP elevation on HCN1 channels, a 6–7-mV positive shift with the tandem dimers, and a 15-mV shift with HCN2. These values are consistently lower than the shifts that we directly observed in cell-free patches or inferred from the intact oocytes. Such a discrepancy, however, is explained by our finding that the basal activation
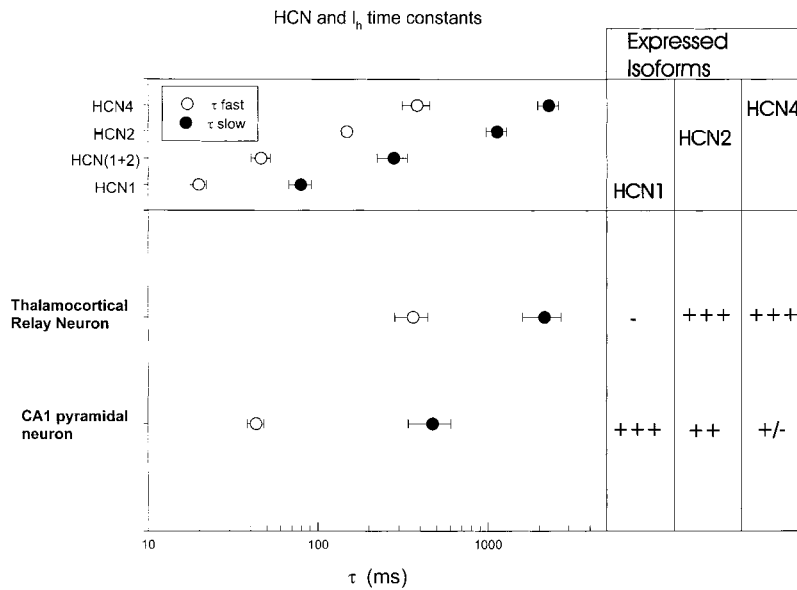
HCN and I_h time constants

Expressed Isoforms

	HCN1	HCN2	HCN4
HCN4			HCN4
HCN2		HCN2	
HCN(1+2)			
HCN1	HCN1		
Thalamocortical Relay Neuron	-	+++	+++
CA1 pyramidal neuron	+++	++	+/-

○ τ fast
● τ slow

τ (ms)

FIGURE 9. Comparison of recombinant and native I_h activation time constants. Fast (τ_{fast}) and slow (τ_{slow}) exponential time constants during activation of I_h for hyperpolarizing steps to -105 mV. Native I_h time constants shown for thalamocortical relay neurons and hippocampal CA1 pyramidal cells from data in Santoro et al. (2000). Relative mRNA expression levels for HCN isoforms from in situ hybridization in corresponding tissues also from Santoro et al. (2000). Data for recombinant HCN1, HCN2, and coexpression of HCN1 + HCN2 from our present study. Time constants normalized to 34°C assuming a Q10 of 4 (DiFrancesco, 1993). Data for rabbit HCN4 taken from Ishii et al. (1999).

curves of HCN channels in intact cells are significantly shifted towards positive potentials by resting levels of cAMP (see following section).

The novel biophysical characteristics of the heteromultimeric channels endow them with unique potential physiological functions. Their relatively positive threshold of activation would allow them to control resting membrane properties and to help generate pacemaker potentials after repolarization of the action potential. Their pronounced modulation by cAMP would contribute to alterations in cellular excitability by hormones and transmitters. These properties of the heteromultimeric channels correspond well with the properties of certain native I_h as discussed two sections below.

Modulation by Basal Level of Cyclic Nucleotides in Cells

Based on differences in channel properties in cell-free patches versus intact cells, together with the high sensitivity of HCN channels to cAMP, we investigated the possible modulation of HCN channels by basal levels of cyclic nucleotide in the intact oocytes. Mutation of a conserved arginine in the β roll of the cyclic nucleotide binding domain to a glutamate completely prevented the modulatory action of cAMP, without altering normal gating properties of either HCN1 or HCN2 channels in cell-free patches. At the structural level, this result is in good agreement with previous results in CNG channels, where a similar mutation blocked activation by cyclic nucleotide without altering the free energy difference between open and closed states in the absence of the ligand (Tibbs et al., 1998). Thus, these two distinct families of cyclic nucleotide regulated ion channels appear to utilize a conserved mechanism in ligand-gating.

Although the point mutations had no effect on the voltage gating of HCN channels in cell-free patches, we did observe significant differences between the mutant channels and wild-type channels in intact oocytes. The voltage dependence of HCN1 and HCN2 homomeric channels was shifted in the hyperpolarized direction by 7 and 19 mV, respectively. Such shifts are nearly identical to the maximal shifts seen with the binding of saturating concentrations of cAMP to HCN1 and HCN2 wild-type channels in cell-free patches (4 and 17 mV, respectively; Fig. 6). This suggests that the basal level of cAMP in oocytes is sufficient to produce near maximal shifts in gating of wild-type HCN channels. This view is compatible with the observation that the $K_{1/2}$ values of these channels range from 50 to 200 nM (Fig. 6), and that resting cAMP levels in oocytes can be in the micromolar range (Maller et al., 1979). Basal modulation by cAMP levels would enhance the modulatory range of these channels, allowing them to respond either to transmitters that elevate levels of cAMP (e.g., acting through G_s) or to transmitters that reduce basal levels of cAMP (e.g., acting through G_i or stimulation of phosphodiesterase activity). In fact, the slowing of the heart by muscarinic receptor stimulation is thought to involve a hyperpolarizing shift in I_h activation due to such a decrease in basal levels of cAMP (DiFrancesco et al., 1989).

The modulation by basal levels of cAMP, however, accounts for only part of the difference in the $V_{1/2}$ values between wild-type I_h in intact oocytes and inside-out patches. This difference is quite large, amounting to a -47-mV shift for HCN1 and a -57 mV shift for HCN2 ($V_{1/2}$ in inside-out patches minus the $V_{1/2}$ in intact oocytes). Similar shifts are also observed for native I_h currents in cardiac myocytes (DiFrancesco and Mangoni, 1994). Taking away the likely shift produced by endogenous cAMP modulation, the remaining shift of approximately -40 mV remains unexplained. Because this shift

is approximately identical in both HCN1 and HCN2, the underlying mechanism accounting for such a difference must be conserved between the two channels.

Coassembly Is Compatible with the I_h in Native Tissues That Express Both HCN1 and HCN2

Although our results show that HCN1 and HCN2 can efficiently coassemble to form heteromultimers in heterologous expression systems, our experiments do not prove that heteromultimer formation necessarily does occur in native tissues in which the subunits are coexpressed. Unfortunately, a lack of suitable antibodies specific for HCN1 and HCN2 isoforms precludes coimmunoprecipitation experiments. However, a careful comparison of the properties of I_h in native tissues that coexpress HCN1 and HCN2 with the properties of I_h generated by the recombinant HCN gene products reported here does indicate that coassembly in vivo is likely. In Fig. 9, we show data from Santoro et al. (2000) that compare the rapid kinetics of I_h recorded from hippocampal CA1 pyramidal neurons, which express HCN1 and HCN2, with the slower kinetics of I_h recorded from thalamocortical relay neurons, which express HCN2 and HCN4. These data are compared with the kinetics of HCN1 channels, HCN2 channels, rabbit HCN4 channels (Ishii et al., 1999), and the heteromultimeric channels we observed upon coexpression of HCN1 and HCN2. We see that the fast and slow time constants in the CA1 pyramidal neurons differ from the properties of recombinant HCN1 or HCN2 homomeric channels. The data for I_h in the pyramidal neurons are in better agreement with the values obtained here for the HCN1/HCN2 heteromultimers. Clearly, future studies are needed to provide more direct evidence for coassembly in native cells. Recordings from CA1 neurons in mice in which the HCN1 gene has been deleted through homologous recombination (Morozov et al., 2000; Nolan et al., 2000) provides a promising means to assess the contribution of heteromultimeric HCN1/HCN2 channels to native I_h currents and to understand the role of these channels in the electrical excitability of individual neurons, the circuits in which these neurons participate, and the complex behaviors that these circuits mediate.

REFERENCES

Bader, C.R., P.R. Macleish, and E.A. Schwartz. 1979. A voltage-clamp study of the light response in solitary rods of the tiger salamander. *J. Physiol.* 296:1–26.

Beaumont, V., and R.S. Zucker. 2000. Enhancement of synaptic transmission by cyclic AMP modulation of presynaptic Ih channels. *Nat. Neurosci.* 3:133–141.

Brown, H., and D. DiFrancesco. 1980. Voltage-clamp investigations of membrane currents underlying pace-maker activity in rabbit sino-atrial node. *J. Physiol.* 308:331–351.

Brown, H.F., D. DiFrancesco, and S.J. Noble. 1979. How does adrenaline accelerate the heart? *Nature.* 280:235–236.

Demontis, G.C., B. Longoni, U. Barcaro, and L. Cervetto. 1999. Properties and functional roles of hyperpolarization-gated currents in guinea-pig retinal rods. *J. Physiol.* 515:813–828.

DiFrancesco, D. 1993. Pacemaker mechanisms in cardiac tissue. *Annu. Rev. Physiol.* 55:455–472.

DiFrancesco, D., and P. Tortora. 1991. Direct activation of cardiac pacemaker channels by intracellular cyclic AMP. *Nature.* 351:145–147.

DiFrancesco, D., and M. Mangoni. 1994. Modulation of single hyperpolarization-activated channels (i(f)) by cAMP in the rabbit sino-atrial node. *J. Physiol.* 474:473–482.

DiFrancesco, D., P. Ducouret, and R.B. Robinson. 1989. Muscarinic modulation of cardiac rate at low acetylcholine concentrations. *Science.* 243:669–671.

Franz, O., B. Liss, A. Neu, and J. Roeper. 2000. Single-cell mRNA expression of HCN1 correlates with a fast gating phenotype of hyperpolarization-activated cyclic nucleotide-gated ion channels (I_h) in central neurons. *Eur. J. Neurosci.* 12:2685–2693.

Goulding, E.H., J. Ngai, R.H. Kramer, S. Colicos, R. Axel, S.A. Siegelbaum, and A. Chess. 1992. Molecular cloning and single-channel properties of the cyclic nucleotide-gated channel from catfish olfactory neurons. *Neuron.* 8:45–58.

Ishii, T.M., M. Takano, L.H. Xie, A. Noma, and H. Ohmori. 1999. Molecular characterization of the hyperpolarization-activated cation channel in rabbit heart sinoatrial node. *J. Biol. Chem.* 274: 12835–12839.

Jan, L.Y., and Y.N. Jan. 1997. Cloned potassium channels from eukaryotes and prokaryotes. *Annu. Rev. Neurosci.* 20:91–123.

Ludwig, A., X. Zong, M. Jeglitsch, F. Hofmann, and M. Biel. 1998. A family of hyperpolarization-activated mammalian cation channels. *Nature.* 393:587–591.

Ludwig, A., X. Zong, J. Stieber, R. Hullin, F. Hofmann, and M. Biel. 1999. Two pacemaker channels from human heart with profoundly different activation kinetics. *EMBO (Eur. Mol. Biol. Organ.) J.* 18:2323–2329.

Luthi, A., and D.A. McCormick. 1998. H-current: properties of a neuronal and network pacemaker. *Neuron.* 21:9–12.

Magee, J.C. 1999. Dendritic I_h normalizes temporal summation in hippocampal CA1 neurons. *Nat. Neurosci.* 2:848.

Maller, J.L., F.R. Butcher, and E.G. Krebs. 1979. Early effect of progesterone on levels of cyclic adenosine 3′:5′- monophosphate in *Xenopus* oocytes. *J. Biol. Chem.* 254:579–582.

McCormick, D.A., and H.C. Pape. 1990. Properties of a hyperpolarization-activated cation current and its role in rhythmic oscillation in thalamic relay neurones. *J. Physiol.* 431:291–318.

Monteggia, L.M., A.J. Eisch, M.D. Tang, L.K. Kaczmarek, and E.J. Nestler. 2000. Cloning and localization of the hyperpolarization-activated cyclic nucleotide-gated channel family in rat brain. *Brain Res. Mol. Brain Res.* 81:129–139.

Moosmang, S., M. Biel, F. Hofmann, and A. Ludwig. 1999. Differential distribution of four hyperpolarization-activated cation channels in mouse brain. *Biol. Chem.* 380:975–980.

Morozov, A., E. Gibbs, M.F. Nolan, C. Kentros, G. Malleret, B. San-

toro, and E.R. Kandel. 2000. Generation and characterization of mice harboring a knockout of the hyperpolarization-activated channel HCN1. *Soc. Neurosci.* 803.1 (Abstr.).

Nolan, M.F., A. Morozov, E. Gibbs, S.A. Siegelbaum, and E.R. Kandel. 2000. Contribution of HCN1 channels to H-current and membrane properties of CA1 pyramidal neurons. *Soc. Neurosci.* 803.2 (Abstr.)

Pape, H.C. 1996. Queer current and pacemaker: the hyperpolarization-activated cation current in neurons. *Annu. Rev. Physiol.* 58: 299–327.

Santoro, B., and G.R. Tibbs. 1999. The HCN gene family: molecular basis of the hyperpolarization-activated pacemaker channels. *Ann. NY Acad. Sci.* 868:741–764.

Santoro, B., S.G. Grant, D. Bartsch, and E.R. Kandel. 1997. Interactive cloning with the SH3 domain of N-src identifies a new brain specific ion channel protein, with homology to eag and cyclic nucleotide-gated channels. *Proc. Natl. Acad. Sci. USA.* 94:14815–14820.

Santoro, B., D.T. Liu, H. Yao, D. Bartsch, E.R. Kandel, S.A. Siegelbaum, and G.R. Tibbs. 1998. Identification of a gene encoding a hyperpolarization-activated pacemaker channel of brain. *Cell.* 93: 717–729.

Santoro, B., S. Chen, A. Luthi, P. Pavlidis, G.P. Shumyatsky, G.R. Tibbs, and S.A. Siegelbaum. 2000. Molecular and functional heterogeneity of hyperpolarization activated pacemaker channels in the mouse CNS. *J. Neurosci.* 20:5264–5275.

Seifert, R., A. Scholten, R. Gauss, A. Mincheva, P. Lichter, and U.B. Kaupp. 1999. Molecular characterization of a slowly gating human hyperpolarization-activated channel predominantly expressed in thalamus, heart, and testis. *Proc. Natl. Acad. Sci. USA.* 96:9391–9396.

Shabb, J.B., and J.D. Corbin. 1992. Cyclic nucleotide-binding domains in proteins having diverse functions. *J. Biol. Chem.* 267: 5723–5726.

Shi, W., R. Wymore, H. Yu, J. Wu, R.T. Wymore, Z. Pan, R.B. Robinson, J.E. Dixon, D. McKinnon, and I.S. Cohen. 1999. Distribution and prevalence of hyperpolarization-activated cation channel (HCN) mRNA expression in cardiac tissues. *Circ. Res.* 85:1–6.

Southan, A.P., N.P. Morris, G.J. Stephens, and B. Robertson. 2000. Hyperpolarization activated currents in presynaptic terminals of mouse cerebellar basket cells. *J. Physiol.* 526:91–97.

Su, Y., W.R. Dostmann, F.W. Herberg, K. Durick, N.H. Xuong, L. Ten Eyck, S.S. Taylor, and K.I. Varughese. 1995. Regulatory subunit of protein kinase A: structure of deletion mutant with cAMP binding domains. *Science.* 269:807–813.

Tibbs, G.R., D.T. Liu, B.G. Leypold, and S.A. Siegelbaum. 1998. A state-independent interaction between ligand and a conserved arginine residue in cyclic nucleotide-gated channels reveals a functional polarity of the cyclic nucleotide binding site. *J. Biol. Chem.* 273:4497–4505.

Ulens, C., and J. Tytgat. 2001. Functional heteromerization of HCN1 and HCN2 pacemaker channels. *J. Biol. Chem.* 276:6069–6072.

Weber, I.T., and T.A. Steitz. 1987. Structure of a complex of catabolite gene activator protein and cyclic AMP refined at 2.5 A resolution. *J. Mol. Biol.* 198:311–326.

Zagotta, W.N., and S.A. Siegelbaum. 1996. Structure and function of cyclic nucleotide-gated channels. *Annu. Rev. Neurosci.* 19:235–263.